Substructure Versus Property-Level Dispersed Modes Calculation

Eric C. Stewart*, Jeff A. Peck†, T. Jason Bush‡, Clay W. Fulcher§
NASA, Marshall Space Flight Center, AL, 35812

This paper calculates the effect of perturbed finite element mass and stiffness values on the eigenvectors and eigenvalues of the finite element model. The structure is perturbed in two ways: at the "subelement" level and at the material property level. In the subelement eigenvalue uncertainty analysis the mass and stiffness of each subelement is perturbed by a factor before being assembled into the global matrices. In the property-level eigenvalue uncertainty analysis all material density and stiffness parameters of the structure are perturbed modified prior to the eigenvalue analysis. The eigenvalue and eigenvector dispersions of each analysis (subelement and property-level) are also calculated using an analytical sensitivity approximation. Two structural models are used to compare these methods: a cantilevered beam model, and a model of the Space Launch System. For each structural model it is shown how well the analytical sensitivity modes approximate the exact modes when the uncertainties are applied at the subelement level and at the property level.

I. Introduction

Prior to launch, a vehicle undergoes a series of modal tests to validate the structural model. This validation increases confidence in the analysis that directly support a flight design. One analysis that has significant dependance on validated structural models is the design of the flight control system parameters which drive vehicle stability. Flight control system parameters assume a set of bounds based on perturbations in frequencies and modes shapes about the nominal design. For instance, the Ares I-X uncertainty bounds on the first three free-free bending pairs was

- 10-20% in frequency
- +100 inches for node locations
- 20-50% in amplitude[1]

Analytical calculation of the modal dispersions prior to testing is important because it helps define the bounds for the flight control design. Modal dispersion calculations can be costly because they require a solution to the eigenvalue problem for each perturbed design. Modal uncertainty is also problematic because the vehicle model has many parameters to which uncertainty can be applied.

When calculating the modal frequency dispersions the analyst must first decide how to apply the uncertainties. The vehicle model can be dispersed at the integrated vehicle level, at the subelement level, or at the material property level.

Traditionally, modal dispersions are calculated at the integrated vehicle level via an ad hoc method. During the Saturn V, the mode frequencies were determined analytically and then an uncertainty of ±10% was applied on the lower frequencies and ±20% uncertainty was used on the higher order frequencies. The 10%-20% uncertainty rule is based on modal test data and was used to bound the frequency and gain

*AST, Structural Dynamics, NASA MSFC; eric.c.stewart-1@nasa.gov
†AST, Structural Dynamics, NASA MSFC; jeff.peck@nasa.gov
‡Aerospace Engineer, TriVector Services, Inc.; jason.bush@nasa.gov
§Sr. Structural Dynamics Analyst, Jacobs Engineering; clay.w.fulcher@nasa.gov

uncertainties for the flight control system. The mode shape uncertainty calculation was performed by perturbing to the individual degrees of freedom in the model. This method is cheap, but it can lead to non-orthogonal and non-realistic modes. Each nominal mode was multiplied by some uncertainty parameter and the effect of this dispersed mode on the controller was determined. While this "global" modal uncertainty method is computationally cheap, it does not reflect any physics of the problem. Also, the mode shapes and mode frequencies are dispersed independently so the modal uncertainties are uncorrelated to any set of inputs.

Two alternative methods are possible when calculating mode shape and mode frequency dispersions: substructure perturbations and property-level perturbations. Modal dispersions at the subelement level are calculated by applying a factor to the mass and stiffness matrices of each subelement before being assembled into the global matrix. The eigenvalues and eigenvectors of each dispersed model are then easily calculated. The subelement level analysis is computationally expensive, but it provides insight into the uncertainty propagation from the subelement to the integrated vehicle. The property-level analysis takes the subelement analysis and drills down one level farther. Uncertainties are applied to all of the individual material stiffness and mass properties within the integrated model. The property-level method is troublesome for the analyst because there can be thousands of material parameters in a launch vehicle model. Also, it provides no computational savings over the subelement level dispersion. However, the property-level modal analysis lets the engineer apply realistic material uncertainties to the model and it provides insight into the physics of the modal uncertainty analysis.

A method is needed to bring down the high computational cost of the subelement level and part-level modal uncertainty analysis. Analytical sensitivities of the eigenvalues and eigenvectors are defined in the literature. The sensitivities can be calculated using a costly exact method[2] or through a variety of approximate methods.[3–9] An alternative to the analytical sensitivity approximation is structural dynamic modification (SDM) which is shown to be a good approximation when stiffness is the only variable.[10]

Much effort is put forth in the literature to establish a relationship between the applied perturbations at the substructure level and the shift in the frequencies and mode shapes. These studies deal with both subelement level uncertainty propagation[11] and property-level uncertainty propagation.[12,13] However, much of this effort focuses on simple structures like bars, beams, and trusses. While simple structures are helpful at establishing the basis for a technique, a complex model can show the weaknesses in a method by displaying complex physics – such as modal coalescence – not normally present in a simple structure.

This work compares two modal dispersion techniques on both a simple beam model and a complex launch vehicle. On each model, subelement level and part-level uncertainties are applied and the dispersed frequencies and modes shapes are calculated. The frequencies and mode shapes are also approximated using the analytical sensitivities and a first-order Taylor series. Finally, the design variable uncertainties are correlated to the frequency dispersions to determine how subelement uncertainty affects the integrated vehicle.

II. Analysis Techniques

A. Substructure Analysis

A thirty finite element cantilever beam model is used to compare the modal dispersion methods. For the substructure modal dispersion analysis, the beam is divided into five substructures of six elements apiece. Uncertainty factors are then applied to the Young's modulus and material density of each substructure. The global stiffness matrix and mass matrices are represented as a summation of the substructure matrices

$$K = \sum_{i=1}^{N_{SE}} \mu_i k_i \tag{1}$$

$$M = \sum_{i=1}^{N_{SE}} \nu_i m_i \tag{2}$$

where μ_i and ν_i are the applied perturbations and k_i and m_i are the stiffness and mass of the i^{th} substructure.

B. Property-level Analysis

The property-level modal dispersion analysis is very similar to the method described for the substructure analysis. Instead of the uncertainty factor being applied to a substructure of six elements, the uncertainty factors are applied to the individual elements. The global stiffness and mass matrices are then

$$K = \sum_{i=1}^{N_E} \mu_i k_i \tag{3}$$

$$M = \sum_{i=1}^{N_E} \nu_i m_i \tag{4}$$

where k_i and m_i here describe the mass and stiffness of an individual beam element. While the part-level and substructure level global matrices are assembled similarly, the perturbations applied are different for each method.

The part-level modal uncertainty analysis a more complex method only in that it requires more book-keeping for the extra uncertainty factors that are applied to the structure. For a large structural modal like a launch vehicle, this method may lead to thousands of uncertainty factors being applied to the model. Also, the part-level dispersions may have high computational cost as it requires knowledge of the full finite element model and not reduced (i.e. Hurty[14]/Craig-Bampton[15]) models

C. Analytical Sensitivities

The analytical sensitivities of the eigenvectors and eigenvalues are well established, but the basics are described here. The description that follows focuses on the property-level dispersions, but the analysis also applies to the substructure-level analysis.

The eigenvalue problem is formulated as

$$\left.\begin{array}{c} K\phi_i = \lambda_i M \phi_i \\ \phi_i^T M \phi_j = \delta_{ij} \end{array}\right\} \quad i = 1, ..., n \tag{5}$$

By taking the derivatives of the two equations with respect to the design variable x and doing some algebraic manipulation, the sensitivity of the i^{th} eigenvalue with respect to the j^{th} design variable is

$$\frac{d\lambda_i}{dx_j} = \phi_i^T \left(\frac{dK}{dx_j} - \lambda_i \frac{dM}{dx_j} \right) \phi_i \tag{6}$$

The uncertainty factors $\{\mu\}$ and $\{\nu\}$ are grouped together and treated as the vector of independent variables

$$x = \left[\begin{array}{cccccccc} \mu_1 & \mu_2 & \dots & \mu_n & \nu_1 & \nu_2 & \dots & \nu_n \end{array} \right]^T \tag{7}$$

From equations 3-4, we see that

$$\frac{dK}{dx_j} = k_j \tag{8}$$

$$\frac{dM}{dx_j} = m_j \tag{9}$$

so the eigenvalue sensitivity simplifies to

$$\frac{d\lambda_i}{dx_j} = \phi_i^T \left(k_j - \lambda_i m_j \right) \phi_i \tag{10}$$

The eigenvector sensitivity $\frac{d\phi_i}{dx_j}$ is calculated from the equation

$$\left(K - \lambda_i M\right) \frac{d\phi_i}{dx_j} = -\left(\frac{dK}{dx_j} - \lambda_i \frac{dM}{dx_j} - \frac{d\lambda_i}{dx_j} M \right) \phi_i = -\left(k_j - \lambda_i m_j - \frac{d\lambda_i}{dx_j} M \right) \phi_i \tag{11}$$

The value $(K - \lambda_i M)$ is singular and can not be inverted. Many methods are available in the literature to deal with the matrix singularity to get the eigenvector sensitivities. Nelson[2] uses a pseudo-inverse of the singular matrix to solve for the eigenvector derivative. Nelson's method is computationally expensive for large problems since it requires calculation of an $n \times n$ matrix inverse for each of the eigenvectors but it is exact and well-suited for smaller problems. The current analysis uses Nelson's method so that there is no uncertainty in the sensitivity calculations.

Higher-order derivatives are easily calculated from the sensitivity equations. The second derivative[9,16] and of the i^{th} eigenvalue and eigenvector with respect to the j^{th} design variable is

$$\frac{d^2\lambda_i}{dx_j^2} = \frac{d\phi_i^T}{dx_j}\left(\frac{dK}{dx_j} - \lambda_i\frac{dM}{dx_j}\right)\phi_i + \phi_i^T\left(\frac{d^2K}{dx_j^2} - \frac{d\lambda_i}{dx_j}\frac{dM}{dx_j} - \lambda_i\frac{d^2M}{dx_j^2}\right)\phi_i + \phi_i^T\left(\frac{dK}{dx_j} - \lambda_i\frac{dM}{dx_j}\right)\frac{d\phi_i}{dx_j} \quad (12)$$

$$(K - \lambda_i M)\frac{d^2\phi_i}{dx_j^2} = -\left(\frac{d^2K}{dx_j^2} - 2\frac{d\lambda_i}{dx_j}\frac{dM}{dx_j} - \lambda_i\frac{d^2M}{dx_j^2} - \frac{d^2\lambda_i}{dx_j^2}M\right)\phi_i - 2\left(\frac{dK}{dx_j} - \lambda_i\frac{dM}{dx_j} - \frac{d\lambda_i}{dx_j}M\right)\frac{d\phi_i}{dx_j} \quad (13)$$

These expressions are simplified due to the linearity of the stiffness and mass matrices with respect to the design variables because their first derivatives are constant and the second derivatives are zero.

$$\frac{d^2\lambda_i}{dx_j^2} = \frac{d\phi_i^T}{dx_j}\left(k_j - \lambda_i m_j\right)\phi_i - \phi_i^T\left(\frac{d\lambda_i}{dx_j}m_j\right)\phi_i + \phi_i^T\left(k_j - \lambda_i m_j\right)\frac{d\phi_i}{dx_j} \quad (14)$$

$$(K - \lambda_i M)\frac{d^2\phi_i}{dx_j^2} = \left(2\frac{d\lambda_i}{dx_j}m_j + \frac{d^2\lambda_i}{dx_j^2}M\right)\phi_i - 2\left(k_j - \lambda_i m_j - \frac{d\lambda_i}{dx_j}M\right)\frac{d\phi_i}{dx_j} \quad (15)$$

The dispersed modes and frequencies are then calculated using a second-order Taylor series

$$\phi_d = \phi_b + \sum_{j=1}^{n}\frac{d\phi_b}{dx_j}\delta x_j + \frac{1}{2}\frac{d^2\phi_b}{dx_j^2}\delta x_j^2 \quad (16)$$

$$\lambda_d = \lambda_b + \sum_{j=1}^{n}\frac{d\lambda_b}{dx_j}\delta x_j + \frac{1}{2}\frac{d^2\lambda_b}{dx_j^2}\delta x_j^2 \quad (17)$$

where the subscripts d and b indicate the dispersed mode shapes and the baseline mode shapes.

D. Frequency Response Function

A frequency response function (FRF) is used to find the natural frequencies and modal gains and easily show their variations with model perturbations. The FRF works by calculating the transfer function $\hat{H}(\omega)$ for any frequency ω where $\hat{H}(\omega)$ is a relationship of the input force on the structure to the output generalized acceleration at some location. The frequency response function is calculated by starting with the equation of motion, we convert to modal degrees of freedom

$$[I]\{\ddot{\eta}\} + [2\zeta\omega_r]\{\dot{\eta}\} + \left[\omega_r^2\right]\{\eta\} = \{P\} = [\Phi]^T\{F_0\} \quad (18)$$

where ζ is the modal damping of the system, ω_r are the natural frequencies of the system, $[\Phi]$ are the mode shapes of the system, and $\{F_0\}$is the magnitude of the forcing function

$$\{F(t)\} = \{F_0\}\cos(\omega t) \quad (19)$$

The transient response for each of the n modal degrees of freedom is calculated as

$$\eta_r = \eta_{rc}\cos(\omega t) + \eta_{rs}\sin(\omega t) \quad r = 1, 2, ..., n \quad (20)$$

where

$$\eta_{rc} = \frac{\left(\omega_r^2 - \omega^2\right) P_r}{\left(\omega_r^2 - \omega^2\right)^2 + \left(2\zeta_r\omega_r\omega\right)^2} \tag{21}$$

$$\eta_{rs} = \frac{\left(2\zeta_r\omega_r\omega\right) P_r}{\left(\omega_r^2 - \omega^2\right)^2 + \left(2\zeta_r\omega_r\omega\right)^2} \tag{22}$$

$$|\eta_r| = \sqrt{\eta_{rc}^2 + \eta_{rs}^2} = \frac{P_r}{\left(\omega_r^2 - \omega^2\right)^2 + \left(2\zeta_r\omega_r\omega\right)^2}\sqrt{\left(\omega_r^2 - \omega^2\right)^2 + \left(2\zeta_r\omega_r\omega\right)^2} \tag{23}$$

The modal responses are now calculated, the generalized coordinate responses are then calculated from the modal responses as

$$\{x\} = [\Phi]^T \{\eta\} \tag{24}$$

An example of a frequency response function calculation is calculated for a beam with a tip force is applied. The frequency response of the tip displacement and rotation are shown in Figure 1 and Figure 2, respectively. The FRFs clearly show high response to the input force at approximately 1.5 Hz, 8 Hz, and 21.5 Hz.

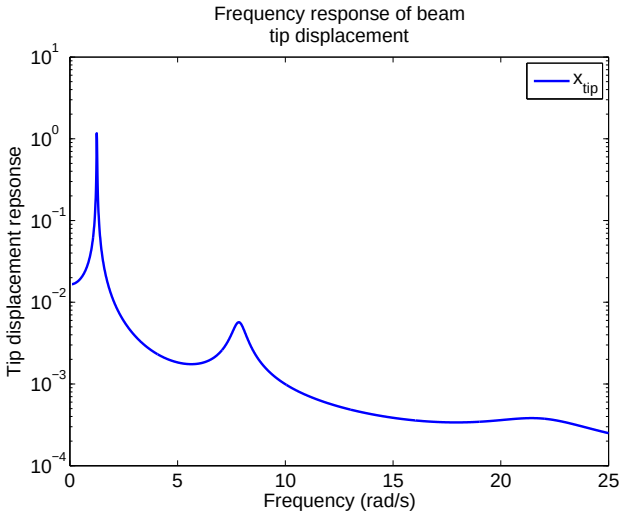

Figure 1. Frequency response of beam tip displacement

E. Modal Assurance Criterion

To investigate the sensitivity of the mode shapes to the subelement and property-level parameters, the modal assurance criterion (MAC)[17] is used. The MAC was developed as a way to compare experimentally-determined mode shapes with analytically-predicted modes. In this work, we use the MAC to compare the dispersed mode shapes to the nominal modes. The modal assurance criterion between two mode shapes is

$$MAC = \frac{\left(\phi_n^T \phi_d\right)^2}{\left(\phi_n^T \phi_n\right)\left(\phi_d^T \phi_d\right)} \tag{25}$$

where ϕ_n is a nominal mode shape and ϕ_d is a dispersed mode shape.

III. Model Dispersion - Beam Model

A. Substructure Analysis

The 30-node beam is divided into five subelements. The mass and stiffness of each subelement is randomly varied with a uniform distribution of $\pm 20\%$ of the nominal value. The eigenvalue problem for each dispersed

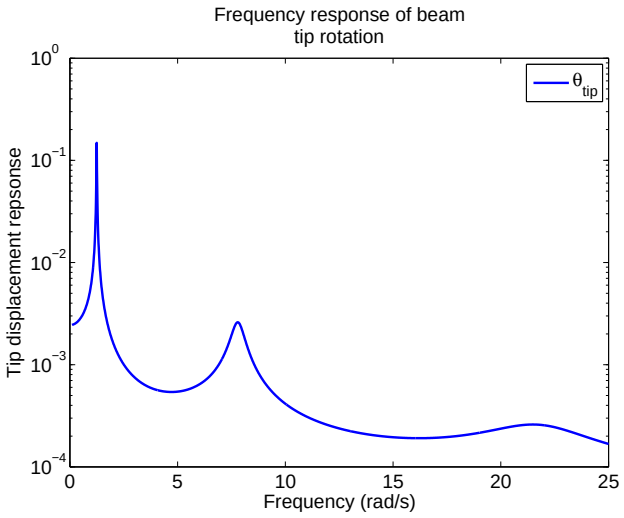

Figure 2. Frequency response of beam tip rotation

beam design is calculated directly using both the MATLAB eigensolver and the analytical sensitivities. The two methods of calculating the eigenvectors are compared in Figs. 3-4.

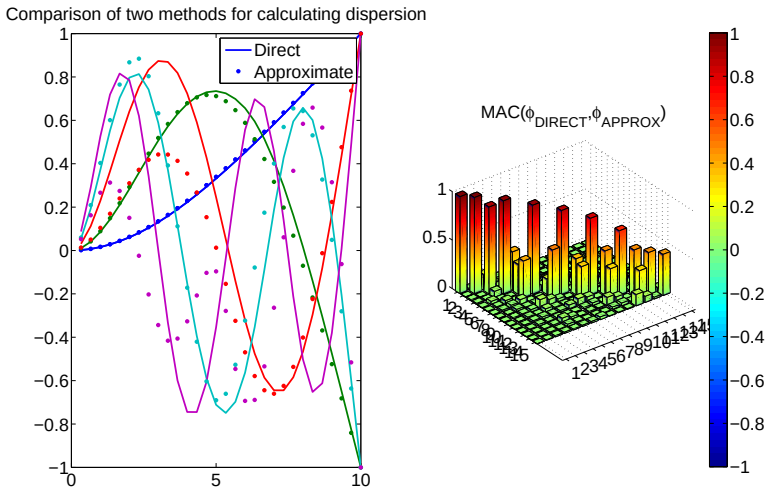

Figure 3. Comparison of beam modes calculated directly and approximated. Uncertainty is applied to the beam substructures.

The two figures compare the modes for two different dispersed cases. The left side of each figure shows the first five eigenvectors calculated directly (solid lines) and approximately (dots). The right side shows the modal assurance criterion comparing the first 15 eigenvectors calculated directly and approximately. For the dispersed design shown in Fig. 3 the eigenvectors calculated via analytical sensitivities do a good job of approximating the lower-order eigenvectors and poorly approximate the higher-order eigenvectors. However, the second dispersed design in Fig. 4 shows that the approximate eigenvectors match the eigenvectors calculated directly from the dispersed mass and stiffness. In the substructure approximation accuracy of the approximate mode shape solution depends highly on the design variables of the dispersed model.

The frequency response function of the 30-element beam model perturbed at the substructure level is shown in Fig. 5 for the directly-calculated modes and in Fig. 6 for the approximate modes. The FRF calculated using the approximated modes shows a good comparison to the exact FRF for the first two

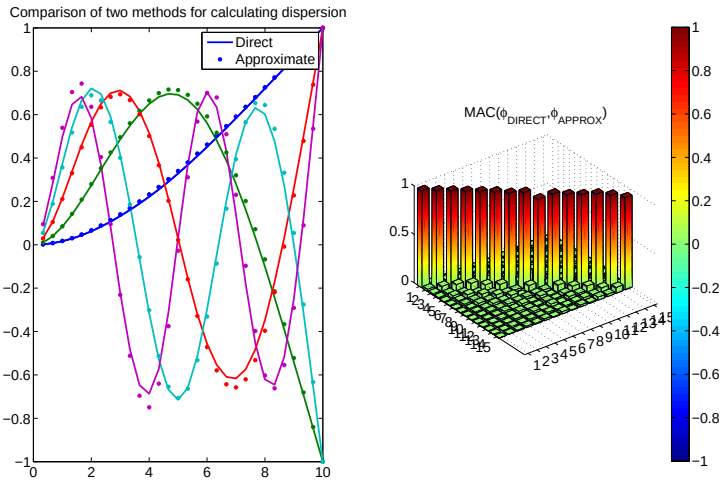

Figure 4. Comparison of beam modes calculated directly and approximated. Uncertainty is applied to the beam substructures.

modes. However, the approximated FRF poorly approximates the exact FRF starting at the third mode. The exact FRF has a gain dispersion from 7.5e-5 to 5e-4 and a frequency dispersion from 3.094 rad/s to 3.956 rad/s whereas the sensitivity approximated FRF has a very tight bound on the gain dispersion and varies in frequency from 3.0517 rad/s to 3.920 rad/s.

The tight uncertainty box around the third mode along with the poor MAC values indicates that the analytical sensitivity solution is not good at approximating the modal dispersions at the substructure level.

The substructure dispersions vary the frequency of the first three FRF peaks by 29%, 24%, and 22%. The large variations in the response peaks is highly undesireable when creating modal dispersions where the goal is a 10% uncertainty on the first mode. While the 20% uncertainty on stiffness and mass could be reduced to get the 10% first mode dispersion, the total uncertainty on a substructure may not be known and the high level of uncertainty ensures conservatism. Thus, part-level dispersions should be used to ensure realistic response variations due to model perturbations.

B. Part-Level Analysis

Now we look at the modal dispersions when the uncertainty factors are applied to the individual elements. For the part-level analysis at the mass and stiffness of each element is randomly varied up to 10% from the nominal. The tighter bounds on the property-level perturbations are because material properties are generally well-known and thoroughly tested. The modes shapes calculated directly from the dispersed modes are compared to the sensitivity approximated modes as shown in Fig. 7. The figure shows the dispersed beam design for which the approximated modes do the worst job at calculating the mode shapes. Even this worst case, defined via the summation of the MAC diagonal for any given case, the exact modes are approximated well by the analytical sensitivity modes.

The part-level dispersed frequency response functions show similar trends to the substructure level dispersed FRFs. The first two FRF peaks match, but the exact FRF in Fig. 8 and the approximated FRF in Fig. 9 do not match at the third peak. The approximated FRF in Fig. shows little gain sensitivity to the mode at 3.5rad/s.

The part-level dispersions vary the frequency of the first three FRF peaks by 11.7%, 11.6%, and 9.3%. These values, particularly the first peak dispersion, are more applicable to creating modal dispersions for GN&C.

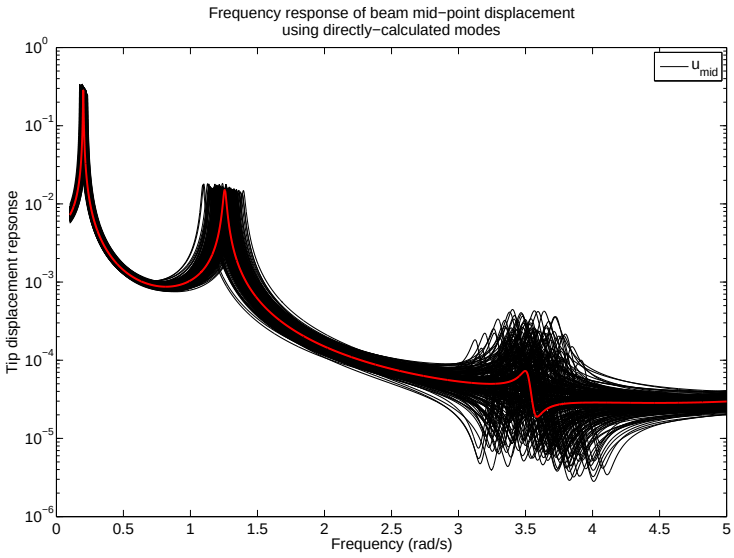

Figure 5. Beam FRF using modes calculated directly using MATLAB eigensolver

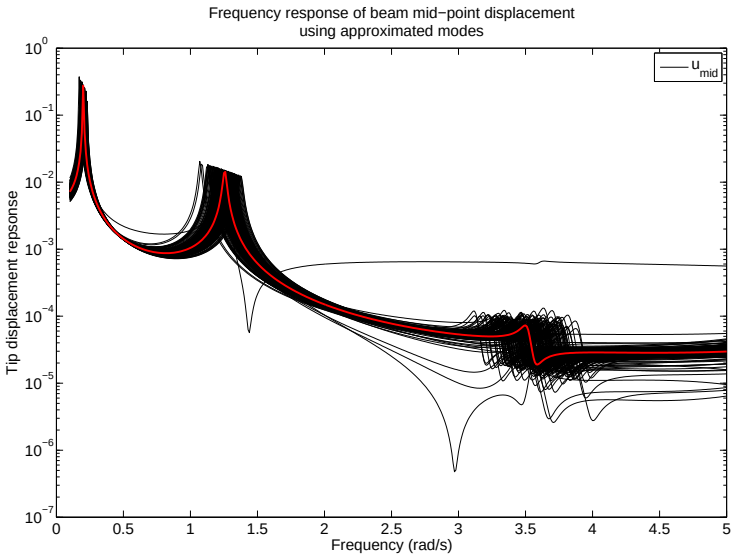

Figure 6. Beam FRF using modes calculated with analytical sensitivities and Taylor series approximation

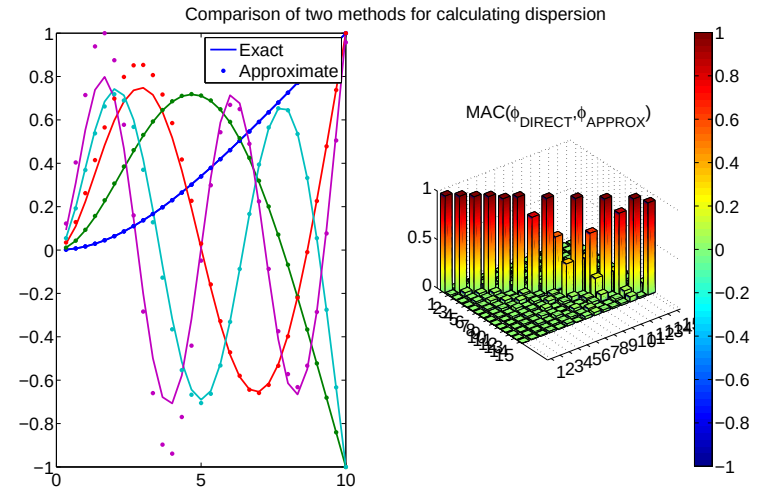

Figure 7. Comparison of beam modes calculated directly and approximated. Uncertainty is applied to the beam individual elements.

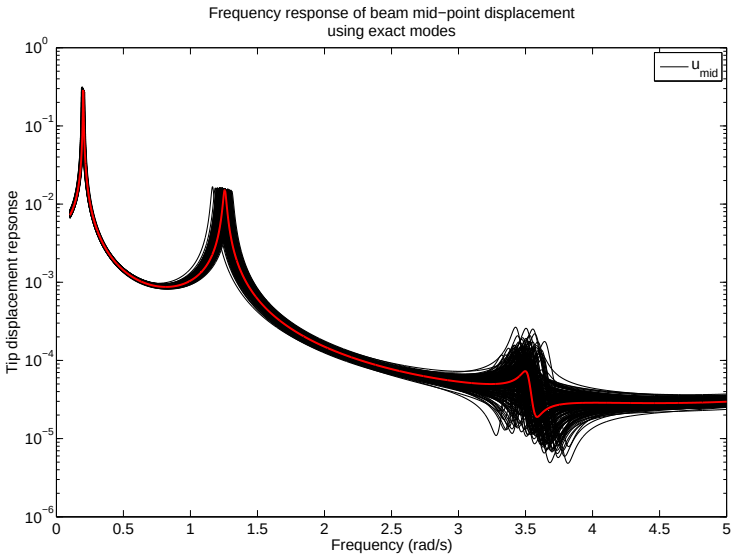

Figure 8. Frequency response function of the beam model with uncertainties applied at part level and eigenvectors calculated directly

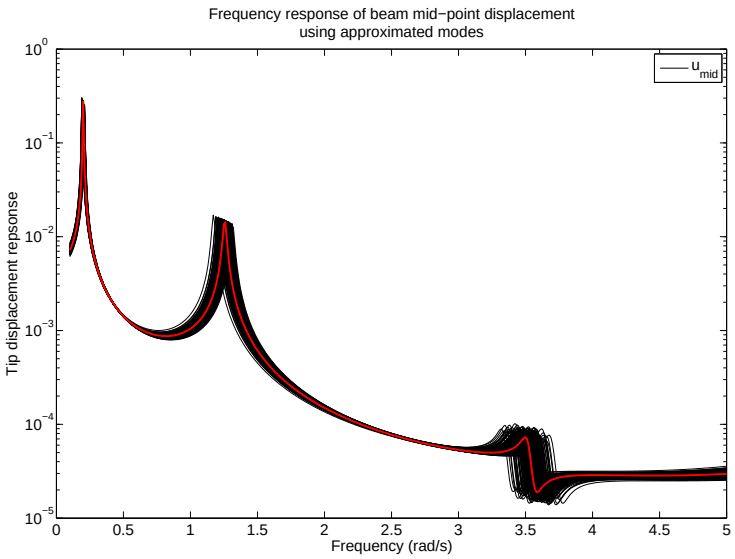

Figure 9. Frequency response function of the beam model with uncertainties applied at part level and eigenvectors calculated with sensitivity analysis

IV. Model Dispersion - TAURUS-T Model

The Test Article Unit for Rectified Systems Testing (TAURUS-T, hereafter referred to as TAURUS) is a simple Unistrut apparatus used as an educational tool at Johnson Space Center. The TAURUS structure is shown in Fig. 10. A NASTRAN model of the TAURUS is created that models the Unistrut as bar elements and the bracket interfaces as springs. The nominal spring constants are determined by modeling the brackets separately and subjecting them to various loading cases. The TAURUS is bolted down and is assumed to be in a fixed-free configuration. The first 10 mode frequencies of the nominal model are shown in Table 1 and compared with the experimentally-determined frequencies.

Table 1. Table of TAURUS modes, both analytical and test

Test Modes (Hz)	Model Modes (Hz)
4.92	3.36
6.60	5.02
7.59	5.65
28.99	27.06
29.35	27.85
31.42	30.88
34.73	38.46
41.09	43.82
43.77	47.14
49.59	49.92

It is noted that for the TAURUS dispersions, analytical sensitivities and eigenvector approximations were not calculated due to time constraints.

Figure 10. The TAURUS structure at Johnson Space Center

A. Substructure Analysis

The TAURUS is modeled as four substructures as shown in Fig. 11. The spring elements within a single substructure are associated with that substructure during model dispersions, but any spring element that touches substructure 4 is dispersed with substructure 4.

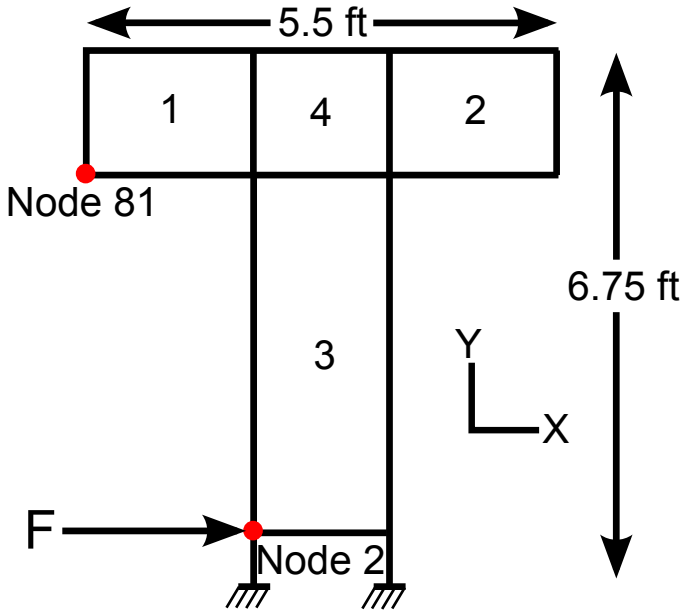

Figure 11. TAURUS with force input node, response output node, and four substructures

For the substructure dispersions, the Young's modulus and spring rates within a substructure are varied ±10% to cover the overall uncertainty in the model stiffness, and the material density is varied ±10% to cover mass uncertainty. The Young's modulus and spring rates within a substructure are varied together and the density is varied independently.

The first 10 modes for each dispersion are calculated and the FRF is calculated where the force is applied to node 2 in the x axis and the response is calculated at node 81 in the x axis. The FRF of the model dispersions is shown in Fig. 12 with the nominal frequency response shown in red. The frequency dispersions on the FRF peaks at 3.36 Hz, 5.65 Hz, and 27.85 Hz are 25%, 25%, and 22%, respectively.

B. Part-Level Analysis

For the part-level dispersions, the Young's modulus and density remain constant while the bar element – which model the Unistrut – cross sectional dimensions are varied by 5% and the spring rates are varied 50%-200% of the nominal values. Young's modulus and density are held constant since material constants tend to stay close to the manufacturer's specifications. Cross-sectional area dimensions are varied so as to provide some variations in the dispersed models. The spring rates are varied with such large values because interface stiffness is notoriously difficult to characterize on many structures and that difficulty is present in the TAURUS model.

Again using the first 10 modes, the FRFs of the part-level dispersions are calculated and shown in Fig. 13. The frequency dispersions on the FRF peaks at 3.36 Hz, 5.65 Hz, and 27.85 Hz are 11%, 11%, and 16%, respectively.

V. Discussion and Conclusions

Three methods of creating mode dispersions were shown in this paper: part-level, substructure, and analytical sensitivities.

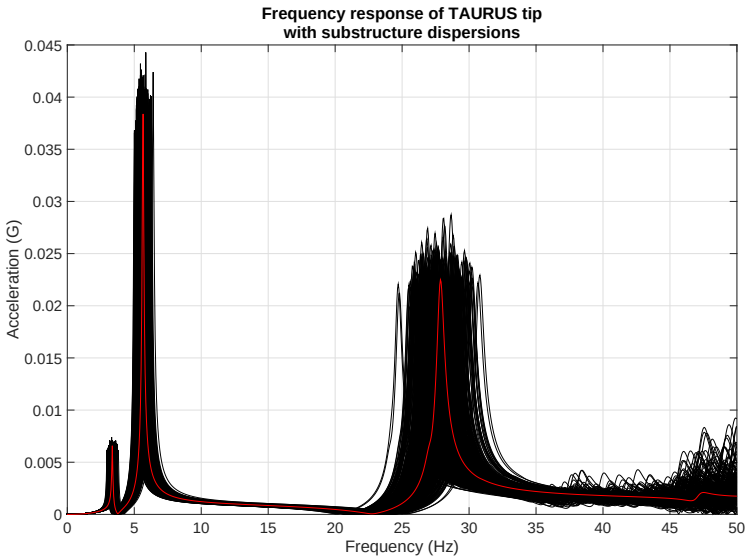

Figure 12. TAURUS FRF with substructure dispersions

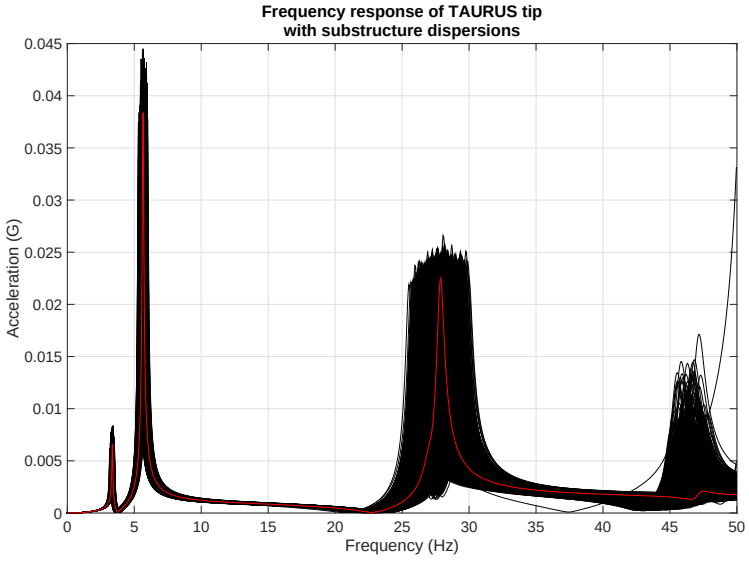

Figure 13. TAURUS FRFs with part-level dispersions

The part-level analysis applies the uncertainty distribution to the material properties and cross-sectional dimensions of the individual finite elements. Part-level modal dispersions are easily implemented when the either the model has a small number of part-level property values or the user has codes to disperse a large number of property values. The part-level dispersion analysis allows the user to apply physically realistic model uncertainty values. So engineering judgment can be used to decrease uncertainty of a property where knowledge of the structure is more well known. The knowledge of the structure means that the model dispersions will have less variation from the nominal and will be physically realistic than substructure dispersions. The part-level dispersions may have high computational cost as it requires knowledge of the full finite element model. However, part-level dispersions should be used if computational cost is a non-factor and the user has access to the full finite element model.

The substructure dispersion analysis takes groups of finite elements and treats them as single substructure. The substructure stiffness and mass are then scaled before assembling into the global mass and stiffness matrices. The substructure-level dispersions should be used when the user does not have knowledge of the full finite element model. This case is particularly true in the aerospace industry, where complex aircraft and launch vehicles necessitates the use of reduced models. While the substructure dispersion analysis is not as physically realistic as the part-level dispersions, it provides some insight into how the mode shapes and frequencies vary in a correlated fashion.

The analytical sensitivity dispersions use the eigenvector and eigenvalue sensitivities to the changes in the global mass and stiffness and then uses a Taylor series expansion to extrapolate the sensitivities and produce model dispersions. The analytical sensitivity dispersions can be used with either the part-level dispersions or the substructure dispersions. The sensitivity modes closely approximate the dispersions in some instances while poorly approximating other dispersions. This is likely due to the breakdown in the Taylor-series approximation to the eigenvectors. The analytical sensitivities provide a method of dispersing the modes if the cost of running an eigenvalue analysis is very high. The user may calculate only the nominal eigenvectors and eigenvalues directly along with the parameter sensitivities.

The analysis in this paper used two structures: a 30 element beam and the TAURUS-T. Future work will focus on incorporating this analysis into model dispersions of complex structures like a launch vehicle. Future investigations will also explore how to improve the analytical sensitivity approximation of the modes.

References

[1]Tuttle, R. E., Hwung, J. S., and Lollock, J. A., "Identifying Goals for Ares 1-X Modal Testing," *Proceedings of the IMAC-XXVIII*, Jacksonville, FL, February 1-4 2010.

[2]Nelson, R. B., "Simplified Calculation of Eigenvector Derivatives," *AIAA Journal*, Vol. 14, No. 9, September 1976, pp. 1201–1205.

[3]Fox, R. L. and Kapoor, M. P., "Rates of Change of Eigenvalues and Eigenvectors," *AIAA Journal*, Vol. 6, No. 12, December 1968, pp. 2426–2429.

[4]Wang, B., "Improved Approximate MMethod for Computing Eigenvector Derivatives in Structural Dynamics," *AIAA Journal*, Vol. 29, No. 6, 1990, pp. 1018–1020.

[5]Beliveau, J.-G., Cogan, S., Lallement, G., and Ayer, F., "Iterative Least-Squares Calculation for Modal Eigenvector Sensitivity," *AIAA Journal*, Vol. 34, No. 2, 1996, pp. 385–391.

[6]Zhang, O. and Zerva, A., "Iterative MMethod for Calculating Derivatives of Eigenvectors," *AIAA Journal*, Vol. 34, No. 5, 1996, pp. 1088–1090.

[7]Alvin, K. F., "Efficient Computation of Eigenvector Sensitivities for Structural Dynamics," *AIAA Journal*, Vol. 35, No. 11, 1997, pp. 1760–1766.

[8]Zheng, S., Ni, W., and Wang, W., "Combined Method for Calculating Eigenvector Derivatives with Repeated Eigenvalues," *AIAA Journal*, Vol. 36, No. 3, March 1998, pp. 428–431.

[9]Smith, D. E. and Siddhi, V., "Generalized Approach for Incorporating Normalization Conditions in Design Sensitivity Analysis of Eigenvectors," *AIAA Journal*, Vol. 44, No. 11, 2006, pp. 2552–2561.

[10]Yap, K. C. and Zimmerman, D. C., "A Comparitive Study of Structural Dynamic Modification and Sensitivity Method Approximation," *Mechanical Systems and Signal Processing*, Vol. 16, No. 4, 2002, pp. 585–597.

[11]Kammer, D. C. and Krattiger, D., "Propagation of Uncertainty in Substructured Spacecraft Using Frequency Response," *AIAA Journal*, Vol. 51, No. 2, 2013, pp. 353–361.

[12]Collins, J. D. and Thomson, W. T., "The Eigenvalue Problem for Structural Systems with Statistical Properties," *AIAA Journal*, Vol. 7, No. 4, 1968, pp. 642–648.

[13]Kiefling, L. A., "Comment on "The Eigenvalue Problem for Structural Systems with Statistical Properties"," *AIAA Journal*, Vol. 8, No. 7, 1970, pp. 1371–1372.

[14]Hurty, W. C., "Dynamic Analysis of Structural Systems Using Component Modes," *AIAA Journal*, Vol. 3, No. 4, April 1965, pp. 678–685.

[15]Craig, R. R. and Bampton, M. C. C., "Coupling of Substructures for Dynamic Analysis," *AIAA Journal*, Vol. 6, No. 7, July 1968, pp. 1313–1319.

[16]Friswell, M. I., "Calculation of Second and Higher Order Eigenvector Derivatives," *Journal of Guidance, Control, and Dynamics*, Vol. 18, No. 4, 1995, pp. 919–921.

[17]Allemang, R. J., "The Modal Assurance Criterion - Twenty Years of Use and Abuse," *Sound and Vibration*, August 2003, pp. 14–21.